한국동력기계공학회지 제19권 제6호 pp. 5-11 2015년 12월 ISSN 1226-7813(Print) ISSN 2384-1354(Online)
Journal of the Korean Society for Power System Engineering http://dx.doi.org/10.9726/kspse.2015.19.6.005
Vol. 19, No. 6, pp. 5-11, December 2015

Dynamic Force Analysis of the 6-DOF Parallel Manipulator

Yoshito Tanaka*, So-Nam Yun***† , Yasunobu Hitaka**,
Masahiro Wakiyama**, Eun-A Jeong***, Ji-U Kim***,
Jung-Ho Park***and Young-Bog Ham***

(Received 30 July 2015, Revision received 17 November 2015, Accepted 18 November 2015)

Abstract: The 6DOF (degrees of freedom) Parallel Manipulators have some advantages that are high power, high rigidity, high precision for positioning and compact mechanism compared with conventional serial link manipulators. For these Parallel Manipulators, it can be expected to work in the new fields such that the medical operation, high-precision processing technology and so on. For this expectation, it is necessary to control the action reaction pair of forces which act between the Parallel Manipulator and the operated object. In this paper, we analyze the dynamics of the 6DOF Parallel Manipulator and present numerical simulation results.

Key Words : Force Analysis, 6-DOF Parallel Manipulator, Dynamic Characteristics, Simulation

1. Introduction

Fig. 1 is a type of the parallel manipulator that is called "Stewart Platform"[1~3]. It consists of a top plate, a bottom plate, and 6 cylinders attached to the top and bottom plates. The top plate is called "platform", and the bottom is called "base".

The platform can be achieved six degrees of freedom motion by six cylinders stretching. The characteristic of this manipulator is that the work space is narrow compared with conventional serial link manipulators. However, Stewart Platform has many advantages that are high power, highrigidity, positioning accuracy and compact mech-anism[4,5]. Then it can be expected to work in the fields by taking advantages of these features. For these purposes, the force control for manipulator of Stewart Platform type is necessary[6,7]. Thus, we analyze about the dynamic forces of this manipulator.

This paper consists of 6 sections. This sectionis introduction. In 2nd section, kinematics of the par-allel manipulator is discussed. In 3rd section, we consider the forces which act on the platform. And then, in section 4, we will analyze the dynamic of parallel manipulator. In section 5, we show the numerical simulation results. Finally, summary is described in section 6.

***† So-Nam Yun (corresponding author) : Department of Extreme Energy Systems, Korea Institute of Machinery & Materials.
E-mail : ysn688@kimm.re.kr, Tel : 042-868-7155
*Yoshito Tanaka : Korea Brain Pool Researcher, Korea Institute of Machinery & Materials.
**Yasunobu Hitaka, Masahiro Wakiyama : Department of Control and Information Engineering , Kitakyusyu National College Technology.
***Eun-A Jeong, Ji-U Kim, Jung-Ho Park, Young Bog-Ham : Department of Extreme Energy Systems, Korea Institute of Machinery & Materials

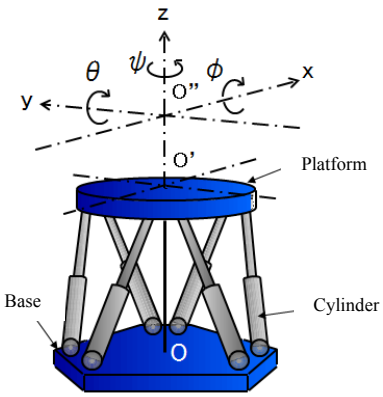

Fig. 1 Parallel manipulator

2. Kinematics of the Parallel manipulator

Fig. 2 is a relationship diagram for the vectors of the parallel manipulator[8,9]. This manipulator has two reference frames. The one is the motion frame and the other is the base fixed frame. The motion frame is located at the centroid O' of the platform, while the base fixed frame has its origin at the centroid O of the base of the manipulator. The attitude of the platform is specified by the orientation of the motion frame and the position of the centroid O' is located with respect to the base fixed frame. The right part of Fig. 2 focuses the vectors related to the i-th cylinder (i=1,...,6). The position of the centroid O' is represented by vector $\mathbf{R} = (x, y, z)^T$ with respect to the base fixed frame. The vector $\mathbf{A}_i$ denotes the attachment point of the cylinder on the platform and the vector B_i denotes attachment point on the base of the manipulator with respect to the base fixed frame. Then, the cylinder length vector $\mathbf{l}_i$ can be calculated by

$$\mathbf{l}_i = \mathbf{A}_{im}\mathbf{T} + \mathbf{R} - \mathbf{B}_i \tag{1}$$

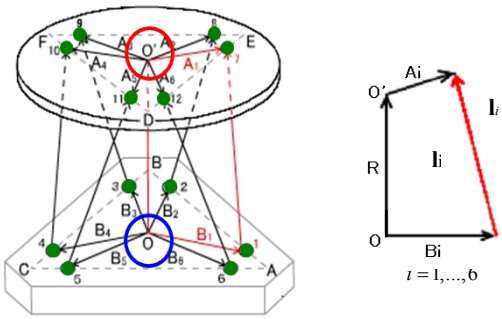

Fig. 2 Vector diagram of parallel manipulator

where $\mathbf{A}_{im}$ describes the attachment point of the cylinder on the platform relative to the motion frame and $\mathbf{T}$ is the oriental matrix of the platform which can be represented by

$$\mathbf{T} = \begin{bmatrix} 1 & 0 & 0 \\ 0 & \cos\phi & \sin\phi \\ 0 & -\sin\phi & \cos\phi \end{bmatrix} \times \begin{bmatrix} \cos\theta & 0 & -\sin\theta \\ 0 & 1 & 0 \\ \sin\theta & 0 & \cos\theta \end{bmatrix} \begin{bmatrix} \cos\psi & \sin\psi & 0 \\ -\sin\psi & \cos\psi & 0 \\ 0 & 0 & 1 \end{bmatrix} \tag{2}$$

with roll-pitch-yaw angles as ϕ, θ and ψ. These angles are around the basis vectors of the motion frame.

3. The forces act on the platform

Fig. 3 is the force analytical model of the parallel manipulator. As shown in this diagram, the platform are acted three types of force, cylinder force $\mathbf{F}_i(i = 1,...,6)$, an external force $\mathbf{L}$ and gravity force $\mathbf{M}$. We consider these force vectors having coordinates $\mathbf{F}_i(F_{ix}, F_{iy}, F_{iz}, i = 1,...,6)$, $\mathbf{L}(L_x, L_y, L_z)$ and $\mathbf{M}(0,0,-mg)$ with respect to the base fixed frame, respectively. Where m is the mass of the platform and g is the gravity acceleration.

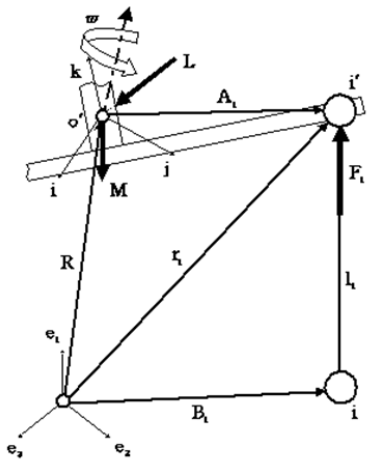

Fig. 3 Analytical model of parallel manipulator

If the motion frame and base fixed frame are ex-pressed by $(\mathbf{i},\mathbf{j},\mathbf{k})^T$ and $(\mathbf{e}_1,\mathbf{e}_2,\mathbf{e}_3)^T$, respectively, the relations among two frames can be described as

$$(\mathbf{i},\mathbf{j},\mathbf{k})^T = \mathbf{T}(\mathbf{e}_1,\mathbf{e}_2,\mathbf{e}_3)^T$$

where, $\mathbf{T}^T = \mathbf{T}^{-1}$ is given because the oriental matrix $\mathbf{T}$ is orthogonal transformation matrix. Then, for the cylinder force $\mathbf{F}_i$, the following relationships

$$(F_{ix}, F_{iy}, F_{iz}) = (F_{i1}, F_{i2}, F_{i3})\mathbf{T} \tag{3}$$

can be obtained, where (F_{i1}, F_{i2}, F_{i3}) is a coordinate of the vector $\mathbf{F}_i$ with respect to the motion frame.

Furthermore, when the coordinate of the i-th cylinder vector $\mathbf{l}_i$ is represented by (l_{ix}, l_{iy}, l_{iz}) with respect to the base fixed frame, we obtain a relation.

$$(F_{ix}, F_{iy}, F_{iz}) = \frac{\mathbf{F}_i}{\sqrt{l_{ix}^2 + l_{iy}^2 + l_{iz}^2}} (l_{ix}, l_{iy}, l_{iz})\,\mathbf{T}^T \tag{4}$$

By Eq.3 and 4, the coordinate (F_{i1}, F_{i2}, F_{i3}) can be written by

$$(F_{i1}, F_{i2}, F_{i3}) = \frac{\mathbf{F}_i}{\sqrt{l_{ix}^2 + l_{iy}^2 + l_{iz}^2}} (l_{ix}, l_{iy}, l_{iz})\,\mathbf{T}^T \tag{5}$$

4. Analysis for the platform dynamics

In order to analyze the platform dynamics, the motion of the platform is considered to be divided into two parts. The one is the translational motion and the other is the rotational motion. First, the translational motion of the platform is discussed.

4.1 Analysis for the translational motion

The equation for the translational motion of the centroid O' of the platform is represented as

$$m\frac{d^2\mathbf{R}}{dt^2} = \sum_{i=1}^{6}\mathbf{F}_i + \mathbf{L} + \mathbf{M} \tag{6}$$

with respect to the fixed frame. By using the Eq. 4, which represents the components of the cylinder force vector relative to the base fixed frame, following three dynamical equations can be obtained from Eq.6.

$$\begin{aligned}
m\frac{d^2x}{dt^2} &= \sum_{i=1}^{6}\frac{l_{ix}}{\sqrt{l_{ix}^2 + l_{iy}^2 + l_{iz}^2}}\mathbf{F}_i + L_x \\
m\frac{d^2y}{dt^2} &= \sum_{i=1}^{6}\frac{l_{iy}}{\sqrt{l_{ix}^2 + l_{iy}^2 + l_{iz}^2}}\mathbf{F}_i + L_y \\
m\frac{d^2z}{dt^2} &= \sum_{i=1}^{6}\frac{l_{iz}}{\sqrt{l_{ix}^2 + l_{iy}^2 + l_{iz}^2}}\mathbf{F}_i + L_z - mg
\end{aligned} \tag{7}$$

4.2 Analysis for the rotational motion

Next, let us consider about the rotational motion of the platform. The equation for this motion is given by

$$\frac{d\mathbf{H}}{dt} + \boldsymbol{\omega}\times\mathbf{H} = \sum_{i=1}^{6}\mathbf{A}_{im}\times\mathbf{F} \tag{8}$$

with respect to the motion frame. Where ω denotes the angular velocity vector for the platform and $\mathbf{H}$ is an angular momentum vector. The $\boldsymbol{\omega}$ is

$$\boldsymbol{\omega} = \omega_1\mathbf{i} + \omega_2\mathbf{j} + \omega_3\mathbf{k} \tag{9}$$

with respect to the motion frame.

Where, ω_1, ω_2 and ω_3 in Eq.9 can be described with Euler angle ϕ, θ, ψ and these derivatives $\dot{\phi}, \dot{\theta}, \dot{\psi}$ as

$$\begin{aligned}\omega_1 &= \dot{\phi} - \dot{\psi}\sin\theta \\ \omega_2 &= \dot{\theta}\cos\phi + \dot{\psi}\cos\theta\sin\phi \\ \omega_3 &= -\dot{\theta}\sin\phi + \dot{\psi}\cos\theta\cos\phi\end{aligned} \tag{10}$$

The vector $\mathbf{H}$ can be derived as

$$\mathbf{H} = \begin{bmatrix} H_1 \\ H_2 \\ H_3 \end{bmatrix} = \begin{bmatrix} I_{11} & I_{12} & I_{13} \\ I_{21} & I_{22} & I_{23} \\ I_{31} & I_{32} & I_{33} \end{bmatrix} \begin{bmatrix} \omega_1 \\ \omega_2 \\ \omega_3 \end{bmatrix} \tag{11}$$

where $I_{ij}(i,j=1,2,3)$ denotes the moment of inertia of the platform. Note that we considered the rotating frame of $\boldsymbol{\omega}$ as the motion frame which is fixed the platform and the square matrix for the inertia in Eq.11 is diagonalizable and we obtain following equation

$$\mathbf{H} = \begin{bmatrix} I_{11} & 0 & 0 \\ 0 & I_{22} & 0 \\ 0 & 0 & I_{33} \end{bmatrix} \begin{bmatrix} \omega_1 \\ \omega_2 \\ \omega_3 \end{bmatrix} \tag{12}$$

Therefore, Eq.8 can be rewritten as

$$\begin{bmatrix} \frac{dH_1}{dt} & \frac{dH_2}{dt} & \frac{dH_3}{dt} \end{bmatrix} \begin{bmatrix} \mathbf{i} \\ \mathbf{j} \\ \mathbf{k} \end{bmatrix} + \begin{bmatrix} \mathbf{i} & \mathbf{j} & \mathbf{k} \\ \omega_1 & \omega_2 & \omega_3 \\ H_1 & H_2 & H_3 \end{bmatrix}$$

$$= \sum_{i=1}^{6} \begin{bmatrix} \mathbf{i} & \mathbf{j} & \mathbf{k} \\ a_{i1} & a_{i2} & a_{i3} \\ F_{i1} & F_{i2} & F_{i3} \end{bmatrix} \tag{13}$$

a_{i1}, a_{i2} and a_{i3} are the components of the vector $\mathbf{A}_{im}$ which denotes attachment point of the cylinder on the platform relative to the motion frame. The elements for Eq.13 can be de-scribed as

$$\begin{aligned} I_1\frac{d\omega_1}{dt} + (I_3 - I_2)\omega_2\omega_3 &= \sum_{i=1}^{6} \frac{l_{ix}}{\sqrt{F_{ix}^2 + F_{iy}^2 + F_{iz}^2}}\mathbf{F}_i + L_x \\ I_2\frac{d\omega_2}{dt} + (I_1 - I_3)\omega_3\omega_1 &= \sum_{i=1}^{6} \frac{l_{iy}}{\sqrt{F_{ix}^2 + F_{iy}^2 + F_{iz}^2}}\mathbf{F}_i + L_y \\ I_3\frac{d\omega_3}{dt} + (I_2 - I_1)\omega_1\omega_2 &= \sum_{i=1}^{6} \frac{l_{iz}}{\sqrt{F_{ix}^2 + F_{iy}^2 + F_{iz}^2}}\mathbf{F}_i + L_z \end{aligned} \tag{14}$$

For above equations, let us rewrite F_{i1}, F_{i2} and F_{i3} to the cylinder force $\mathbf{F}_i$ with the relation in Eq.5, the following equations can be obtained.

$$\begin{aligned} & I_1\frac{d\omega_1}{dt} + (I_3 - I_2)\omega_2\omega_3 \\ &= \sum_{i=1}^{6} \frac{a_{i2}\left(l_{ix}T_{31} + l_{iy}T_{32} + l_{iz}T_{33}\right)}{\sqrt{l_{ix}^2 + l_{iy}^2 + l_{iz}^2}}\mathbf{F}_i \\ &- \sum_{i=1}^{6} \frac{a_{i3}\left(l_{ix}T_{21} + l_{iy}T_{22} + l_{iz}T_{23}\right)}{\sqrt{l_{ix}^2 + l_{iy}^2 + l_{iz}^2}}\mathbf{F}_i \\ & I_2\frac{d\omega_2}{dt} + (I_1 - I_3)\omega_3\omega_1 \\ &= \sum_{i=1}^{6} \frac{a_{i3}\left(l_{ix}T_{11} + l_{iy}T_{12} + l_{iz}T_{13}\right)}{\sqrt{l_{ix}^2 + l_{iy}^2 + l_{iz}^2}}\mathbf{F}_i \\ &- \sum_{i=1}^{6} \frac{a_{i1}\left(l_{ix}T_{31} + l_{iy}T_{32} + l_{iz}T_{33}\right)}{\sqrt{l_{ix}^2 + l_{iy}^2 + l_{iz}^2}}\mathbf{F}_i \\ & I_3\frac{d\omega_3}{dt} + (I_2 - I_1)\omega_1\omega_2 \\ &= \sum_{i=1}^{6} \frac{a_{i1}\left(l_{ix}T_{21} + l_{iy}T_{22} + l_{iz}T_{23}\right)}{\sqrt{l_{ix}^2 + l_{iy}^2 + l_{iz}^2}}\mathbf{F}_i \\ &- \sum_{i=1}^{6} \frac{a_{i3}\left(l_{ix}T_{11} + l_{iy}T_{12} + l_{iz}T_{13}\right)}{\sqrt{l_{ix}^2 + l_{iy}^2 + l_{iz}^2}}\mathbf{F}_i \end{aligned} \tag{15}$$

$T_{ij}(i, j = 1,2,3)$ in Eq.15 is the element of the oriental matrix $\mathbf{T}$.

Therefore, the dynamics of the 6DOF parallel manipulator can be described by six differential equations in Eq.7 and 15.

5. Simulation

In this section, we provide the numerical simulation based on our analysis. Fig. 4 shows the 6DOF parallel manipulator used in the simulation. (a) is appearance of experimental apparatus and (b) is top view of 6-cylinders arrangement. The main specifications of the mechanism used for the calculation are given in Table 1.

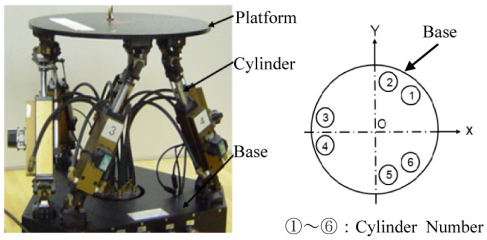

(a) Appearance of parallel manipulator (b) Arrangement of 6-cylinders

Fig. 4 6DOF hydraulic parallel manipulator

Fig. 5 shows the calculation results for the surge motion $(x = \pm 90mm)$ as an example in transitional motion of the platform.

Fig. 6 shows the calculation results for the yaw motion $(\psi = \pm 30\,\mathrm{deg}.)$ as an example in rotational motion of the platform.

In Fig. 5 and 6, (a) denotes the amount of the cylinder stretch and (b) denotes the cylinder force amount for six cylinders. Where, "Cylinder number" denotes cylinder of the parallel manipulator in Fig. 4, and the lateral axes of both diagrams in Fig. 5, 6 indicate the movements for the centroid O' of the platform.

Table 1 Main specification of the mechanism

x :mm	±90	A_{i2}:mm	(50.5,167.5,-60.0)
y : mm	±90	A_{i3}:mm	(-170.3,40.0,-60.0)
z : mm	±50	A_{i4}:mm	(-170.3,-40.0,-60.0)
ϕ : deg	±18	A_{i5}:mm	(50.5,-167.5,-60.0)
θ : deg	±18	A_{i6}:mm	(119.8,-127.5,-60.0)
ϕ : deg	±30	B_{i1}:mm	(221.4,40.0,50.0)
m:kg	4.0	B_{i2}:mm	(-76.0,211.7,50.0)
I_{11}:kgmm^2	44100	B_{i3}:mm	(-145.3,171.7,50.0)
I_{22}:kgmm^2	44100	B_{i4}:mm	(-145.3,-171.7,50.0)
I_{33}:kgmm^2	88200	B_{i5}:mm	(-76.0,-211.7,50.0)
A_{i1}:mm	(119.8,127.5.-60.0)	B_{i6}:mm	(221.4,--40.0,50.0)

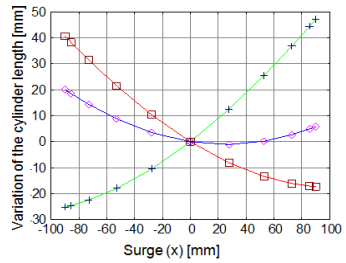

(a) The amount of the cylinder stretch

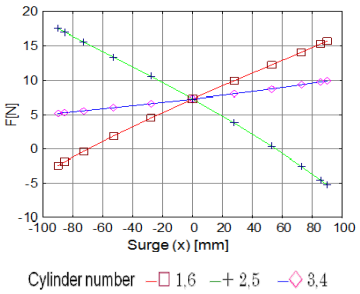

(b) The cylinder force for six cylinders.

Fig. 5 The calculation results for the surge motion $(x = \pm 90mm)$

Fig. 7 shows the thrust forces of each cylinders in motional sinusoidal frequency 1Hz. (a) is the surge sinusoidal motion; (b) is the yaw sinusoidal motion, respectively. Fig. 5(b) and Fig. 6(b) shows 0.5Hz in motional sinusoidal frequency.

From Fig. 5(b) and Fig. 7(a), Fig. 6(b) and Fig. 7(b), when movement of platform is running fast, the thrust forces of each cylinder is can be seen that it is necessary to larger force.

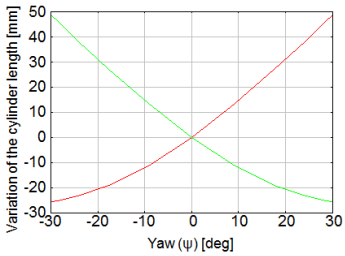

(a) The amount of the cylinder stretch

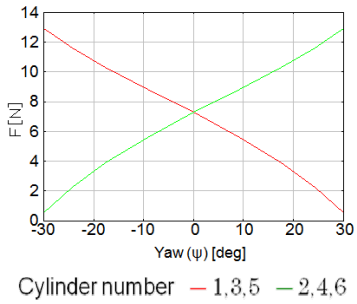

(b) The cylinder forces for six cylinders

Fig. 6 The calculation results for the yaw motion ($\psi = \pm 30\,\mathrm{deg.}$)

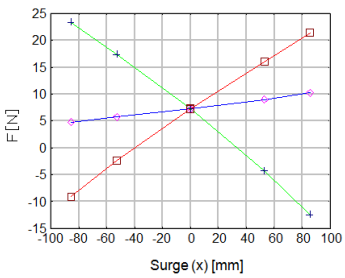

(a) Surge motion

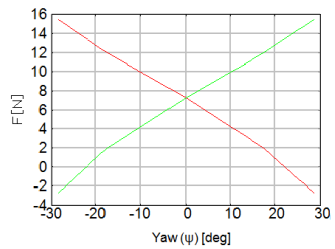

(b) Yaw motion

Fig. 7 Thrust forces of each cylinders in motional frequency 1Hz

6. Summary

In this paper, we analyzed the dynamics force of the 6DOF parallel manipulator and showed the numerical simulation results.

From simulation results, it has become possible to predict each cylinder force required for dynamic movements of the platform.

By this analysis method, dynamic force analysis of a variety of multi-degree- of-freedom parallel manipulator becomes possible, and can be used as a future of design support tool.

In our future work, we'll confirm our analysis by experiment for the actual. Experiment is required to confirm the validity of the simulation results.

And moreover, we'll utilize our analytical result to the force control in order that the parallel manipulator can be useful in many fields such that the medical operation, high-precision processing technology and so on.

Acknowledgement

This research was financially supported by the 2014 Brain Pool Program of the KOFST (MF054A).

References

1. D. Stewart, 1965, “A platform with six degrees of freedom”, Proc. Instn. Mech. Engrs, Vol. 180-1-15, pp. 371-378.
2. Hiroaki Funahashi, 1992, “Parallel Mechanisms As a New Robotic Mechanism”, JRSJ Vol. 10, No. 6, pp. 699-704.
3. M. T. Kandakure, V. G. Gaikar and A. W. Patwardhan, 2005, “Hydrodynamic aspects of ejectors, Chemical Engineering Science”, Vol. 60, No. 3, pp. 6391-6402.

4. Sarah. F, Karl-Peter J and Ansgar. T, 2014, "Test Rig for the Hardware-in-the-Loop Simulation of Mechatronic Axles", 9th IFK 2014 in Aachen, pp. 366-377.
5. I. Y . Lee, 1998, "Trend of Hydraulic Servo Control Technology-Topics on Automobile Application", Journal of KSPSE, Vol. 2, No. 1, pp. 10-16.
6. Takaiwa. M, Noritsugu T, 1999, "Development of Human-Robot Haptic Interface Using Pneumatic Parallel Manipulator", Proc. 4th JHPS Int. Symp. on Fluid Power, pp. 181-186.
7. Tanaka. Y, Nakajima. T, Sawada. T, 2003, "Desktop Type of Force Display Using Pneumatic Parallel Mechanism", Proceedings of the Fourth International Symposium on Fluid Power Transmission and Control (ISFP'2003, Paper for Plenary Session), pp. 267-271.
8. Koichi Sugimoto, 1992, "Force Analysis for Parallel Manipulators", JRSJ Vol. 10, No. 6, pp. 706-708.
9. Kazuhiro Kosuge, Okuda Minoru, et al., 1994, "Input/output Analysis of Parallel Link Manipulator", JSME Vol. 60, No. 675, pp. 134-140.